

Hadron freeze-out conditions in high energy nuclear collisions

Nu Xu and Masashi Kaneta

Lawrence Berkeley National Laboratory, Berkeley, CA 94720, USA

1. Introduction

The purpose of the current heavy ion programs at CERN (Switzerland) and Brookhaven National Laboratory (USA) is to probe strongly interacting matter under extreme conditions, i.e. at high densities and temperatures. The central subject of these studies is the transition from the quark-gluon plasma to hadronic matter. In the early phases of ultra-relativistic heavy ion collisions, when a hot and dense region is formed in the center of the reaction, there is copious production of up, down, and strange quarks. Transverse expansion is driven by the multiple scattering among the incoming and produced particles. As the medium expands and cools, the quarks/gluons combine to form the hadrons that are eventually observed.

In June 2000, the long awaited gold collisions were delivered by the RHIC collider at $\sqrt{s_{\text{NN}}} = 130$ GeV. A great amount of new data, analyzed from that brief period of running, was presented at this conference [1–4]. From SPS, results on the systematic of the transverse momentum distributions of ϕ [5] and J/ψ [6,7] were shown. New results from 40 and 80 A·GeV ($\sqrt{s_{\text{NN}}} \approx 9$ and 12 GeV) [8,9] collisions were also shown.

In this paper, we will summarize the recent experimental results on transverse momentum distributions and particle ratios. The related physics issues are chemical equilibrium and collective expansion. While the former has to do with the inelastic collisions, the later is dominated by the elastic cross section. We will focus at the relatively low transverse momentum region, $p_t \leq 2$ GeV/c, where the bulk production occurs. For results on high momentum transfer, global measurements, and correlations readers are referred to [10–12].

2. Kinetic freeze-out: transverse momentum distributions

At this conference, identified particle transverse momentum distributions at mid-rapidity were shown by the BRAHMS, PHENIX, and STAR experiments [1,2,4,13,14]. While PHENIX measured π , K , and p up to 2.5 GeV/c in p_t , the STAR TPC provided clean spectra of identified particles up to about 1 GeV/c in p_t within a somewhat wider rapidity window. The preliminary transverse momentum distributions for negative pions, kaons, and anti-protons from the STAR Collaboration are shown in Fig. 1. The results are from the 6% most central Au+Au collisions. Hydrodynamic motivated fits are also shown in the figure as dashed lines [15]. The extracted common freeze-out temperature and collective velocity parameters are about 100 MeV and $0.6c$, respectively. In Fig. 2, the preliminary transverse momentum distribution of anti-protons from the PHENIX collaboration [13]

is compared to the STAR results [14]. It is important to note that the transverse momentum distributions are consistent within the overlap region. Below $m_t - \text{mass} = 0.7$ GeV/c^2 , both sets of data are consistent with the hydrodynamic fit. The lower part of the distribution is from the NA44 Collaboration at SPS ($\sqrt{s_{\text{NN}}} = 17.2$ GeV) [16].

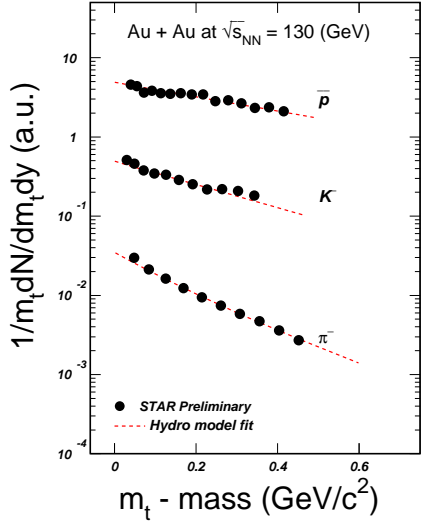


Figure 1 The STAR preliminary results of the transverse mass distributions for negative pions, kaons, and anti-protons from Au+Au central collisions. Dashed lines represent the model fit results.

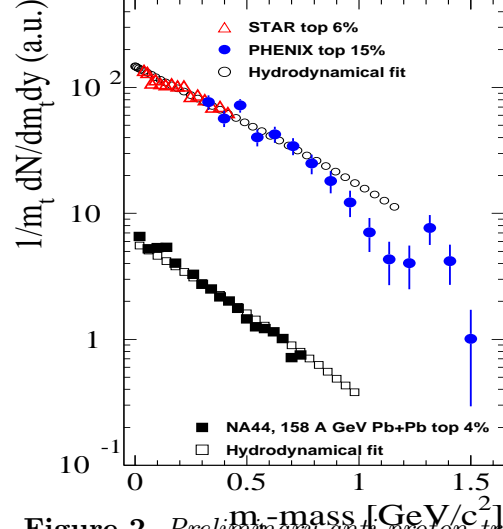


Figure 2 Preliminary anti-proton transverse mass distributions from STAR and PHENIX (circles) are compared. Squares represent the results from central Pb+Pb collisions. Open symbols represent the model fit results.

The measured transverse momentum distributions also have been fitted by the exponential function $f = A \cdot \exp(-m_t/T)$, where T is the slope parameter and A is the normalization constant. The magnitude of the slope parameter provides information on temperature (random motion in local rest frame) and collective transverse flow. Fig. 3(a) shows the measured particle slope parameters from Pb+Pb central collisions at SPS ($\sqrt{s_{\text{NN}}} = 8.8$ GeV and $\sqrt{s_{\text{NN}}} = 17.2$ GeV) energies [8,9,16,17]. The new results are:

- Particle distributions from 40 A· GeV ($\sqrt{s_{\text{NN}}} = 8.8$ GeV) collisions were reported by NA45 and NA49 [8,9]. The slope parameters are similar to the ones observed at 158A· GeV, *i.e.*, they follow the established systematic trend [18];
- For the first time, the systematic of the transverse momentum distributions for charm particles (J/ψ) was reported by the NA50 experiment [6,7]. It is interesting to note that the slope parameter of J/ψ is similar to those for ϕ and Ω ;
- For central collisions the ϕ slope parameter of NA49 is about 300 MeV [5] whereas that of the NA50 is about 240 MeV. NA49 and NA50 reconstructed ϕ mesons via K^+K^- and $\mu^+\mu^-$ channels, respectively. As discussed in [19,20], part of the difference may be caused by the final state interaction of the decay kaons. In fact, if one studies the centrality dependence of the ϕ slope parameter, one finds that at

peripheral collisions, both experimental results agree with each other and the value is close to that from $p + p$ collisions [5,6].

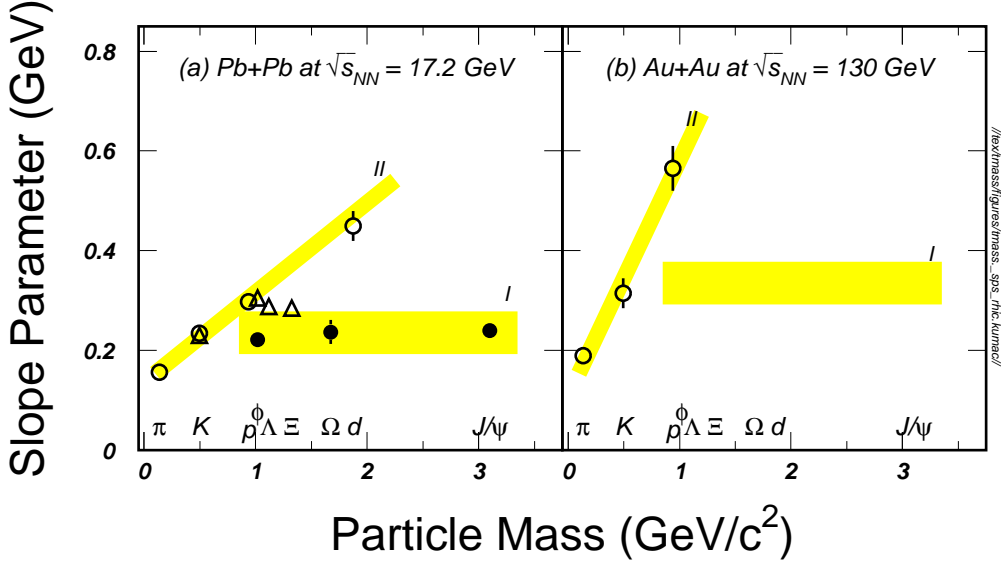


Figure 3 Slope parameters as a function of particle mass for (a) Pb+Pb central collisions at SPS ($\sqrt{s_{NN}} = 17.2$ GeV) and Au+Au central collisions at (b) RHIC ($\sqrt{s_{NN}} = 130$ GeV). Weak and strong interacting limits are indicated by I and II, respectively.

Preliminary results of the slope parameters from Au+Au central collisions at RHIC ($\sqrt{s_{NN}} = 130$ GeV) [4,14] are shown in Fig. 3(b). It is obvious that the mass dependence of the slope parameter is stronger than that from collisions at SPS energies.

As one can see from Fig. 3(a), the slope parameters appear to fall into two groups: group (I) is flat as a function of particle mass, whereas the slopes in group (II) increase strongly with particle mass. At the RHIC energy, the slope parameter systematic of π , K , and p shows an even stronger dependence on the particle mass. The strong energy dependence of the slope parameter might be the result of the larger pressure gradient at the RHIC energy. With a set of reasonable initial/freeze-out conditions and equation of state, the stronger transverse expansion at the RHIC energy was, in deed, predicted by hydrodynamic calculations [21–23]. In addition, the results are consistent with the large value of the event anisotropy parameter v_2 at the RHIC energy [24,25].

Within the hadronic gas, the interaction cross section for particles like ϕ , Ω , and J/ψ are smaller than that of π , K , and p [26]. Therefore the interactions between them and the rest of the system are weak, leading to the flat band behavior in Fig. 3(a). On the other hand, the slope parameter of these weakly interacting particles may reflect some characteristics of the system at hadronization. Then it should be sensitive to the strength of the color field [27–29]. Under this assumption, the fact that the weak interacting particles show a flat slope parameter as a function of their mass would indicate that the *flow* develops at a later stage of the collision. Should the collective flow develop at the partonic level, one would expect a mass dependence of the slope parameters for all particles [30].

Based on the idea of Color Glass Condensate, McLerran and Schaffner-Bielich predicted [31] that the measured mean p_t is controlled by the intrinsic p_t broadening rather

than transverse flow. It will be interesting to see the slope parameters of ϕ , Ω , and J/ψ from collisions at RHIC energies. As indicated by the horizontal bar in Fig. 3(b), one might expect both the absolute magnitude and the slope as a function of particle mass to be different from that observed at SPS energies.

Figure 4 shows the bombarding energy dependence of the freeze-out temperature T_{fo} and the average collective velocity $\langle\beta_t\rangle$. It is interesting to observe that both T_{fo} and $\langle\beta_t\rangle$ saturate at a beam energy of about 10 A·GeV. The saturation temperature is about 100 - 120 MeV, very close to the mass of the lightest meson [32]. The steep rise of the T_{fo} and $\langle\beta_t\rangle$ up to about 5 A·GeV incident energy indicates that at low energy collisions the thermal energy essentially goes into kinetic degrees of freedom. The saturation at ~ 10 A·GeV shows that particle generation becomes important. As proposed in [32,33], for a pure hadronic scenario there may be a limiting temperature $T_c \approx 140$ MeV in high-energy collisions, although the underlying physics for both, the transition from partonic to hadronic degrees of freedom and the transition from interacting hadrons to free-streaming is not clear at the moment. By coupling the limiting temperature idea to a hydrodynamic model calculation, Stöcker *et al.* successfully predicted [34] the energy dependence of the freeze-out temperature. It is worth noting that measurements of the pion phase density [35–37] at freeze-out also show saturation at $E_{beam} \sim 10$ A·GeV.

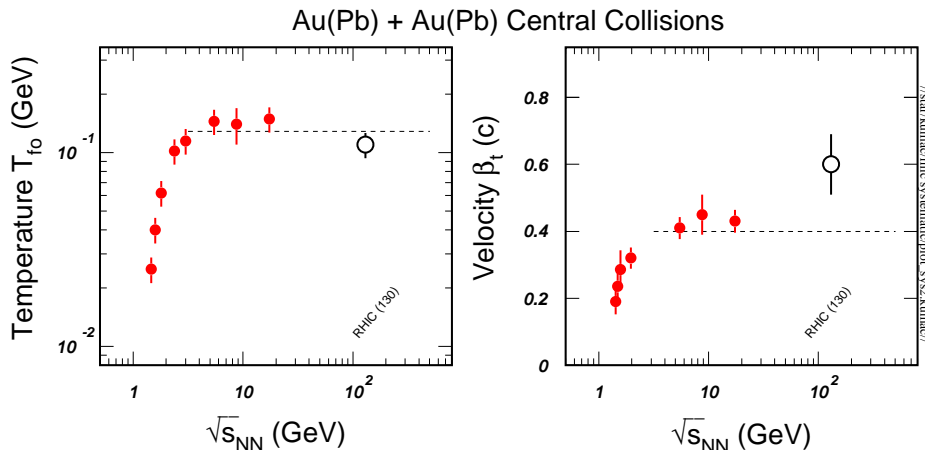


Figure 4 Systematics of kinetic freeze-out temperature parameter T_{fo} and average collective transverse flow velocity $\langle\beta_t\rangle$ as a function of beam energy. At $\sqrt{s_{NN}} \approx 5$ GeV, both values of temperature and velocity parameters seem to saturate. However, the velocity parameter extracted from central collisions at the RHIC energy is higher than values from collisions at lower beam energies.

At the RHIC energy, the collective velocity parameter seems to be larger than that from collisions at AGS/SPS energies. This can already be seen in Fig. 3 where the increase from pion to proton at $\sqrt{s_{NN}} = 130$ GeV (Fig. 3(b)) is much faster than at $\sqrt{s_{NN}} = 17$ GeV (Fig. 3(a)). Is this the manifestation of van Hove's [38] picture? On the other hand, compared to results from lower energy collisions, the temperature parameters seem to be lower. Is this the consequence of hydrodynamic expansion [39] from a higher initial density fireball? An energy scan between $\sqrt{s_{NN}} = 20 - 130$ GeV will be extremely important in order to study this evolution in more detail.

3. Mid-rapidity \bar{p}/p ratios and net-proton distributions

All RHIC experiments have consistently measured the ratio of \bar{p}/p at mid-rapidity [40–44]. The dependence of the \bar{p}/p ratios as a function of the center of mass energy is shown in Fig. 5. Only central collision results were used for heavy ion collisions. Clearly, although the ratio is not unity, a dramatic increase in the ratio is observed from SPS to RHIC, meaning that the system created at $\sqrt{s_{NN}} = 130$ GeV is close to net-baryon free.

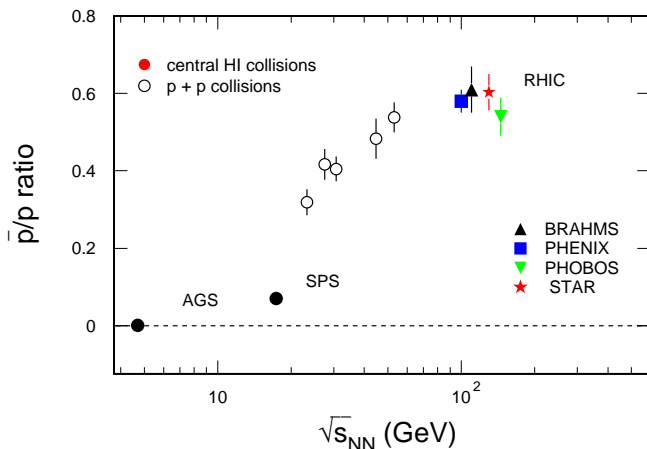


Figure 5 Mid-rapidity \bar{p}/p ratios measured in central heavy-ion collisions (filled symbols) and $p + p$ collisions (open symbols). The left end of the abscissa is the $p - \bar{p}$ pair production threshold in $p + p$ ($\sqrt{s_{NN}} = 3.75$ GeV).

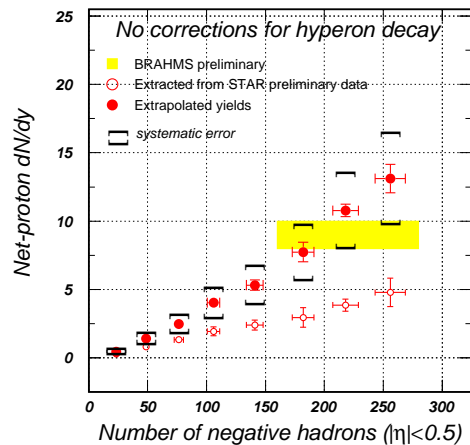


Figure 6 Net-protons yields as a function of charge particle multiplicity. Open and filled symbols represent the yields within $0.3 \leq p_t \leq 1.0$ GeV/c and the values extracted from the full transverse momentum range, respectively. No hyperon decay corrections have been applied to the yields.

One of the unsolved problems in high energy nuclear collisions is the baryon transfer that occurs at the early stage of the collision [45]. The later dynamic evolution of the system is largely determined at this moment since the available energy is fixed at this stage of the collision. On the theoretical side, a novel mechanism, the non-perturbative gluon junction, was proposed to address this problem [46,47]. From the STAR measured \bar{p}/p ratios [40] and the STAR preliminary results of anti-proton yields [4], we have extracted the net-proton yields at mid-rapidity. The values are shown in Fig. 6 as a function of collision centrality. Open symbols represent the measured yields within $|y| \leq 0.1$ and $0.3 \leq p_t \leq 1.0$ GeV/c. The fill symbols show the values extracted from the full transverse momentum range. Estimated systematic uncertainties are shown as caps. No hyperon decay corrections have been applied as that requires the knowledge of the yields of hyperons. The hatched bar represents the BRAHMS preliminary results [1].

One can see that the number of net protons increase as the number of the negatively charged particles increases. This implies that more and more protons (baryons) are transferred from the incoming nuclei to mid-rapidity as the overlap of the two nuclei increases. More data are needed to study the role of the junction mechanism [46,47] in heavy ion collisions. In this respect, the rapidity distributions of the net-protons as a function of

collision centrality will be of crucial importance.

4. Chemical freeze-out: particle ratios

Recently, much theoretical effort has been devoted to the analysis of particle production within the framework of statistical models [48,49]. These approaches are applied to the results of both elementary collisions ($e + e^-$, $p + p$) and heavy ion collisions ($Au + Au$ and $Pb + Pb$) [48]. Many features of the data imply that a large degree of chemical equilibration may be reached both at AGS and SPS energies. The three most important results are: (i) at high energy collisions the chemical freeze-out (inelastic collisions cease) occurs at about 160-180 MeV and it is ‘universal’ to both elementary and heavy ion collisions; (ii) the kinetic freeze-out (elastic scatterings cease) occurs at a lower temperature $\sim 120 - 140$ MeV; (iii) the compilation of freeze-out parameters [50] in heavy ion collisions in the energy range from 1 - 200 A-GeV shows that a constant energy per particle $\langle E \rangle / \langle N \rangle \sim 1$ GeV can reproduce the behavior in the temperature-potential ($T_{ch} - \mu_B$) plane [50].

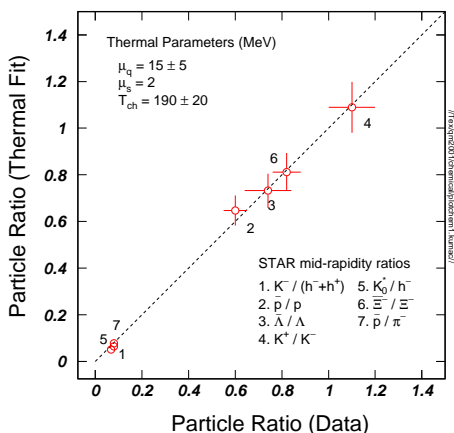


Figure 7 STAR preliminary particle ratios vs. results of thermal model fits. The thermal parameters for temperature and chemical potential are $T_{ch} = 190 \pm 20$ MeV and $\mu_B = 45 \pm 15$ MeV, respectively.

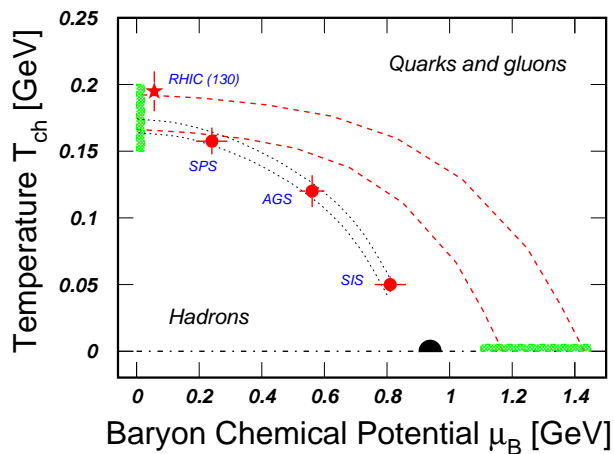


Figure 8 Phase plot T_{ch} vs. μ_B . Dashed-line represents the boundary between interactions involving hadronic and partonic degrees of freedom. Dotted-lines represent the results of [50]. The ground state of nuclei is shown as half circle.

The measured mid-rapidity particle ratios [4,51] were fitted with a statistical model [52] and the results are shown in Fig. 7. The resulting thermal parameters for temperature and baryon potential are $T_{ch} = 190 \pm 20$ MeV and $\mu_B = 45 \pm 15$ MeV, respectively. It is not surprising that the temperature parameter is close to the prediction [53] for RHIC.

The systematics for chemical parameters is shown in the phase plot in Fig. 8 where the dashed lines represent the boundary between interactions involving hadronic and partonic degrees of freedom. The dotted lines represent the results of [50]. Results from heavy ion collisions at SIS, AGS, and SPS energies are shown as circles. The result from collisions at the RHIC energy is shown as star. The lattice prediction on T_c (≈ 160 MeV) is shown at $\mu_B = 0$ and the baryon density for neutron star is indicated at the $T_{ch} = 0$.

There are technical caveats in above approaches. The application of a statistical model requires that the measurement is done over the whole phase-space, *i.e.*, with 4π particle yields. This is because conservation laws that apply to the collisions are only valid for global measurements, *not locally*. In all experiments the coverage of the phase-space is limited. Therefore, extracting the yields measured within limited phase-space to 4π yields is almost impossible, especially for the collider experiments. In addition, we should point out that the non-local effect is common to all global conservation laws (baryon number, charge, and so on), not only to the strangeness.

5. Summary

In summary, the most interesting results from collisions at RHIC are that the system is indeed approaching net-baryon free and the transverse expansion is much stronger than that from collisions at AGS/SPS energies.

In order to understand the trend of the collective velocity, an energy scan between $\sqrt{s_{\text{NN}}} = 20 - 200$ GeV, is important. In addition, systematic studies on the anisotropy parameter v_2 and the transverse momentum distributions of ϕ , Ω , and J/ψ are necessary as they will help in determining whether the collectivity is developed at the partonic stage.

We are grateful for many enlightening discussions with Drs. P. Braun-Munzinger, W. Busza, M. Gyulassy, U. Heinz, B. Holzman, P. Huovinen, B. Jacak, F. Navarra, S. Panitkin, K. Redlich, H.G. Ritter, K. Schweda, E.V. Shuryak, R. Snellings, D. Teaney, F.Q. Wang, and X.N. Wang. This work has been supported by the U.S. Department of Energy under Contract No. DE-AC03-76SF00098.

REFERENCES

1. F. Videbaek *et al.*, (BRAHMS Collaboration), these proceedings.
2. B. Zajc *et al.*, (PHENIX Collaboration), these proceedings.
3. G. Roland *et al.*, (PHOBOS Collaboration), these proceedings.
4. J. Harris *et al.*, (STAR Collaboration), these proceedings.
5. V. Friese *et al.*, (NA49 Collaboration), these proceedings.
6. P. Bordalo *et al.*, (NA50 Collaboration), these proceedings.
7. M.C. Abreu *et al.*, (NA50 Collaboration), Phys. Lett. **B499**, 85(2001).
8. H. Appelshäuser *et al.*, (NA45 Collaboration), these proceedings.
9. C. Blume *et al.*, (NA49 Collaboration), these proceedings.
10. A. Drees, these proceedings.
11. P. Steinberg, these proceedings.
12. S. Panitkin, these proceedings.
13. J. Velkovska *et al.*, (PHENIX Collaboration), these proceedings.
14. Mauel Calderón de la Sánchez *et al.*, (STAR Collaboration), these proceedings.
15. E. Schnedermann, J. Sollfrank, and U. Heinz, Phys. Rev. **C48**, 2462(1993).
16. I. G. Bearden *et al.*, (NA44 Collaboration), Phys. Rev. Lett **78**, 2080(1997); M. Kaneta, Ph.D Thesis, (NA44 Collaboration), March (1999).
17. E. Andersen *et al.*, (WA97 collaboration), Phys. Lett. **B433**, 209(1998).
18. N. Xu *et al.*, (NA44 Collaboration), Nucl. Phys. **A610**, 175c(1996).

19. S. Johnson, B. Jacak, and A. Drees, E. J. Phys. **C**, in print, (2001).
20. S. Soff *et al.*, J. Phys. G: Nucl. Part. **27**, 449(2001).
21. P. Huovinen, these proceedings.
22. D. Teaney, these proceedings.
23. P. Huovinen, P. Kolb, U. Heinz, P.V. Ruuskanen, and S. Voloshin, Phys. Lett. **B503**, 58(2001).
24. K.H. Ackermann *et al.*, (STAR Collaboration), Phys. Rev. Lett. **86**, 402(2001).
25. R. Snellings *et al.*, (STAR Collaboration), these proceedings.
26. H. van Hecke, H. Sorge, and N. Xu, Phys. Rev. Lett. **81**, 5764(1998).
27. J. Schwinger, Phys. Rev. **82**, 664(1951).
28. S. Soff, S. Bass, M. Bleicher, L. Bravina, M. Gorenstein, E. Zabrodin, H. Stöcker, and W. Greiner, Phys. Lett. **B471**, 89(1999).
29. M. Bleicher, W. Greiner, H. Stöcker, and N. Xu, Phys. Rev. **C62**, R1901(2000).
30. R. Thews, M. Schroedter and J. Rafelski, J. Phys. **G27**, 715(2001); R. Thews, M. Schroedter and J. Rafelski, LANL Preprint hep-ph/0007323 v3, Feb. (2001).
31. L. McLerran and J. Schaffner-Bielich, LANL Preprint hep-ph/0101133, Jan. (2001).
32. I.Ya. Pomeranchuk, Dokl. Akad. Sci. U.S.S.R. **78**, 884(1951).
33. R. Hagedorn, Suppl. Nuovo Cim. **III.2**, 147(1965).
34. H. Stöcker, A.A. Ogloblin, and W. Greiner, Z. Phys. **A303**, 259(1981).
35. J. Cramer *et al.*, (STAR Collaboration), QM01, Poster Session.
36. M. Lisa *et al.*, (E895 Collaboration), these proceedings.
37. F. Laue *et al.*, (STAR Collaboration), these proceedings.
38. L. van Hove, Z. Phys. **C21**, 93(1983).
39. F. Navarra, M. Nemes, U. Ornik, and S. Paiva, Phys. Rev. **C45**, R2552(1992); Y. Hama and F. Navarra, Z. Phys. **C53**, 501(1992).
40. C. Adler *et al.*, (STAR Collaboration), Phys. Rev. Lett., in print (2001).
41. I. Bearden *et al.*, (BRAHMS Collaboration), these proceedings.
42. N. George *et al.*, (PHOBOS Collaboration), these proceedings.
43. H. Ohnishi *et al.*, (PHEMIX Collaboration), these proceedings.
44. H. Huang *et al.*, (STAR Collaboration), these proceedings.
45. W. Busza and R. Ledoux, Ann. Rev. Nucl. Part. Sci. **38**, 119(1988).
46. D. Kharzeev, Phys. Lett. **B378**, 238(1996).
47. S. Vance, M. Gyulassy, and X.N. Wang, Phys. Lett. **B443**, 238(1998).
48. P. Braun-Munzinger, J. Stachel, J. Wessels, and N. Xu, Phys. Lett. **B344**, 43(1995); P. Braun-Munzinger, I. Heppe, and J. Stachel, Phys. Lett. **B465**, 15(1999).
49. F. Becattini, M. Gazdzicki, and J. Sollfrank, Eur. Phys. J. **C5**, 143(1998); F. Becattini, Z. Phys. **C69**, 485(1996); F. Becattini and U. Heinz, Z. Phys. **C76**, 269(1997).
50. J. Cleymans and K. Redlich, Phys. Rev. Lett. **81**, 5284(1998).
51. H. Caines *et al.*, (STAR Collaboration), these proceedings.
52. J. Letessier, J. Rafelski, and A. Tounsi, Phys. Lett. **B328**, 499(1994); M. Kaneta *et al.*, (NA44 Collaboration), J. Phys. G: Nucl. Part. Phys. **23**, 1865(1997).
53. J. Stachel, Nucl. Phys. **A661**, 226c(1999); P. Braun-Munzinger and K. Redlich, private communications, (2001).